Biomechanics and Modeling in Mechanobiology
https://doi.org/10.1007/s10237-022-01640-y

ORIGINAL PAPER

The impact of thickness heterogeneity on soft tissue biomechanics: a novel measurement technique and a demonstration on heart valve tissue

Chien-Yu Lin[1] · Mrudang Mathur[2] · Marcin Malinowski[3,4] · Tomasz A. Timek[3] · Manuel K. Rausch[1,5,6]

Received: 13 June 2022 / Accepted: 19 September 2022

Abstract

The mechanical properties of soft tissues are driven by their complex, heterogeneous composition and structure. Interestingly, studies of soft tissue biomechanics often ignore spatial heterogeneity. In our work, we are therefore interested in exploring the impact of tissue heterogeneity on the mechanical properties of soft tissues. Therein, we specifically focus on soft tissue heterogeneity arising from spatially varying thickness. To this end, our first goal is to develop a non-destructive measurement technique that has a high spatial resolution, provides continuous thickness maps, and is fast. Our secondary goal is to demonstrate that including spatial variation in thickness is important to the accuracy of biomechanical analyses. To this end, we use mitral valve leaflet tissue as our model system. To attain our first goal, we identify a soft tissue-specific contrast protocol that enables thickness measurements using a Keyence profilometer. We also show that this protocol does not affect our tissues' mechanical properties. To attain our second goal, we conduct virtual biaxial, bending, and buckling tests on our model tissue both ignoring and considering spatial variation in thickness. Thereby, we show that the assumption of average, homogeneous thickness distributions significantly alters the results of biomechanical analyses when compared to including true, spatially varying thickness distributions. In conclusion, our work provides a novel measurement technique that can capture continuous thickness maps non-invasively, at high resolution, and in a short time. Our work also demonstrates the importance of including heterogeneous thickness in biomechanical analyses of soft tissues.

Keywords Mitral valve · Optical profilometry · Mechanical testing · Biaxial tension · Bending · Buckling

1 Introduction

Characterizing and predicting the mechanical properties of soft tissues is critical to our understanding of health and disease (Ferruzzi et al. 2018; Witzenburg and Holmes 2018; Luetkemeyer et al. 2020). These properties are often driven by soft tissues' complex, heterogeneous composition and structure (Bersi et al. 2019; Farzaneh et al. 2019; Fuentes et al. 2020). That is, soft tissues are usually organized in layers with each layer showing distinct and spatially varying properties. Of course, this is common knowledge (Meador et al. 2020a; Buerzle et al. 2013; Witzenburg and Barocas 2016). It is therefore noteworthy that, with few exceptions, many studies ignore heterogeneity when conducting mechanical analyses of soft tissues, including some of our own (Sree et al. 2019; Sachs et al. 2021; Luetkemeyer et al. 2021). The reason likely being that measuring spatially varying properties is hard and time-consuming, with benefits often unknown. In our current work, we are therefore

Chien-Yu Lin and Mrudang Mathur have contributed equally to this work.

✉ Manuel K. Rausch
manuel.rausch@utexas.edu

[1] Department of Biomedical Engineering, University of Texas at Austin, Austin, TX 78712, USA

[2] Department of Mechanical Engineering, University of Texas at Austin, Austin, TX 78712, USA

[3] Division of Cardiothoracic Surgery, Spectrum Health, Grand Rapids, MI 49503, USA

[4] Department of Cardiac Surgery, School of Medicine in Katowice, Medical University of Silesia, Katowice, Poland

[5] Department of Aerospace Engineering and Engineering Mechanics, University of Texas at Austin, Austin, TX 78712, USA

[6] Oden Institute for Computational Engineering and Sciences, University of Texas at Austin, Austin, TX 78712, USA

Published online: 25 October 2022

interested in exploring and highlighting the impact of tissue heterogeneity on biomechanical analyses of soft tissues. Therein, we specifically focus on soft tissue heterogeneity arising from spatially varying thickness.

Our interest in exploring heterogeneity in tissue thickness was first sparked during a recent computational study of the human tricuspid valve in which we assumed that each leaflet had a uniform thickness (Mathur et al. 2022). We made these assumptions because creating an accurate, spatially varying thickness map appeared non-feasible with our available thickness measurement techniques. In the course of said modeling work, we found that the simulated heart valves folded in rather unnatural locations. Thus, we re-inspected the original tissue and found that native heart valve leaflets tended to be significantly thinner in those regions that undergo folding, while being thicker in those regions that aren't meant to fold. In other words, native tissue had a non-uniform thickness distribution. From an engineering perspective, this is an entirely logical design with thinner areas being a nucleus for folding and buckling (Joda et al. 2016; Lee et al. 2015). To overcome the limitation of our work, we began a quest for a technique to measure spatially varying tissue thickness and to provide strong support for the inclusion of heterogeneity in thickness—and other physical properties—in biomechanical analyses.

Of course, there are many means to measure tissue thickness (O'Leary et al. 2013; Ge et al. 2020). However, none we found fulfilled our need for (1) being non-destructive, (2) having a high spatial resolution, (3) providing continuous spatial maps, and (4) being fast. For example, histology-based methods are destructive and provide thickness measurements only within two-dimensional layers (Ud-Din et al. 2019; Smith et al. 2021), gauges and calipers only provide focal measurements (Chen et al. 2020; Jana and Lerman 2019), while ultrasound has a limited spatial resolution and optical coherence tomography is limited in depth (Moran and Thomson 2020; Aumann et al. 2019; Bersi et al. 2020). The first goal of our work is therefore to introduce a technique that fulfills needs (1)–(4) and to demonstrate this technique on heart valve tissue. Our second goal is to demonstrate the importance of including tissue heterogeneity in biomechanical analyses via virtual planar biaxial tests, bending tests, and a buckling mode analysis; again, by example of heart valve tissue.

2 Methods

2.1 Tissue origin and preparation

We isolated anterior mitral valve leaflets from seven healthy male Dorset sheep, 51 ± 8 kg aged 5–6 months, and cryogenically stored the tissue at − 80 °C in a 9:1 ratio of DMEM:DMSO with protease inhibitor until final testing (Meador et al. 2020b). Immediately before testing, we rapidly thawed the leaflets to room temperature and photographed them while they floated on a layer of 1× PBS. We used a background grid for calibration. Please note that others have found minimal impact of freezing on heart valve tissue properties (Salinas et al. 2020; Duginski et al. 2020).

2.2 Tissue profilometry

After taking photographs of a thawed anterior mitral valve leaflet, we gently dried it using absorbent tissue (KimWipes, Kimberly-Clark, Irving, TX, USA). Next, we covered the tissue with microfine talc granules suspended with a trace of lanolin (PowderPen, NextEngine, CA, USA) to minimize tissue glare and to reduce the tissue's optical transparency. Finally, we created a 3D thickness map of the leaflet using an optical profilometer (VHX-5000, Keyence, Osaka, Japan) under 50× magnification. To validate the accuracy of our tissue profilometry, we also measured the thickness of a rubber sample in multiple regions with a digital thickness gauge (547-500S, Mitutoyo Corp., Kawasaki, Japan) and subsequently imaged the same sample with the Keyence scope to obtain its spatial thickness map for comparison.

2.3 Biaxial testing

To ensure that our profilometry protocol did not have spurious effects on tissue mechanics, we performed repeated biaxial testing on a separate set of tissues: once before and once after powder application, see Fig. 1. Specifically, we isolated a 7 mm × 7 mm square from the belly regions of $n = 6$ anterior mitral valve leaflets. Before mounting the tissues to our planar biaxial tester, we marked the atrialis surface of each sample with ink dots in a 3 mm × 3 mm square pattern. Floating on 1× PBS, we took images of this pattern for later use. Next, we mounted the samples on our biaxial device (Biotester, Cellscale, Waterloo, ON, Canada) and tested the samples twice without dismounting them: First, in 37 °C 1× PBS, after which we gently dried the sample with absorbent tissue (KimWipes) and applied the same powder to the sample as used in preparation for imaging. Subsequently, we let the sample air-dry for 10 min (the length of our imaging protocol), before carefully cleaning the sample with 1× PBS and performing a second set of mechanical tests in 37 °C 1× PBS. Between tests we did not zero the load cells (1.5 N capacity, ± 1.5 mN) and tests began from identical motor positions. During both tests, we performed 10 preconditioning cycles equibiaxially to 500 mN, preloaded the tissue to 10 mN to remove any slack, and then conducted two final equibiaxial cycles to 500 mN. While testing, we recorded the rake-to-rake distances, radial and circumferential forces, and fiducial marker images at 5 Hz.

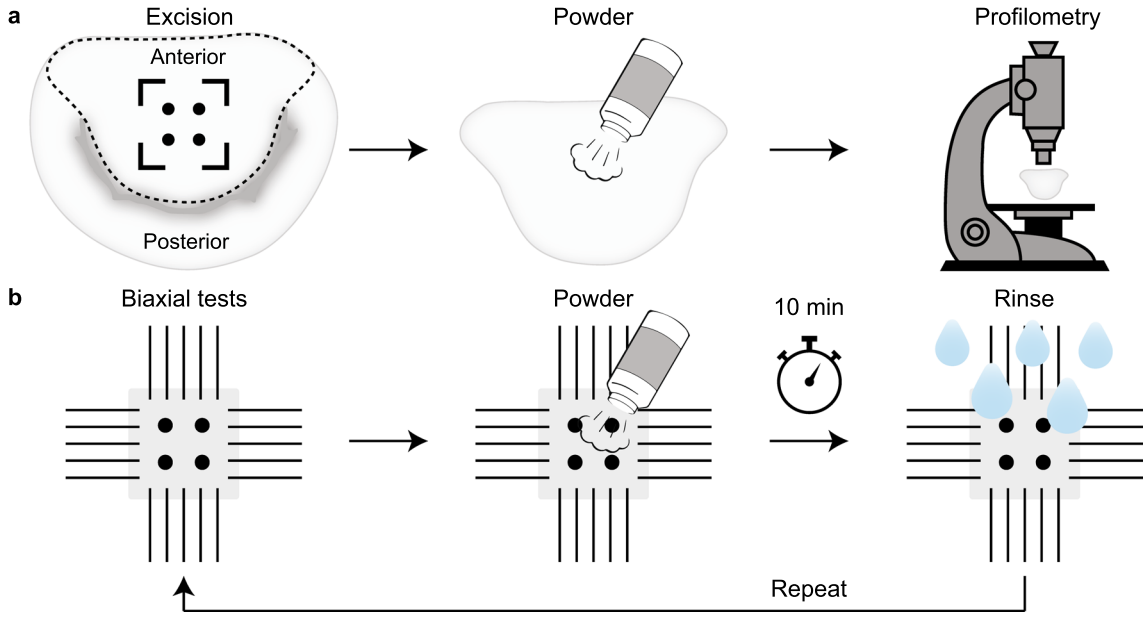

Fig. 1 Experimental overview. **a** We excised the anterior leaflet of an ovine mitral valve and applied talcum powder for optical contrast. Next, we imaged the sample using a Keyence profilometer to create a high-resolution, spatial thickness map of our sample. **b** Next, we tested whether the application of talcum powder and a 10-minute imaging period negatively affects the tissues' mechanics. To this end, we measured the biaxial properties of $n = 6$ additional anterior leaflets before and after applying powder for 10 minutes

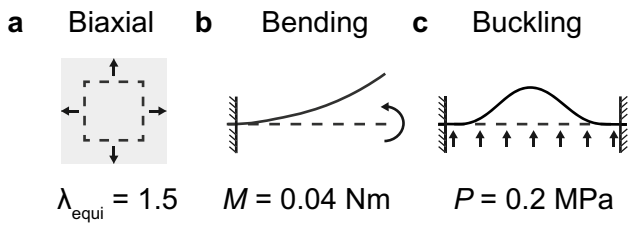

Fig. 2 Loading modes for numerical analyses. We apply **a** displacements to the edge of our samples under biaxial stretch, **b** a moment to the free-edge of our samples under bending, and **c** a perturbation pressure to the surface of our samples under buckling. Please note, dashed lines indicate the reference configuration

Using the fiducial marker positions on the tissue throughout testing, we calculated the deformation gradient tensor, $\mathbf{F}$, with respect to the floating stress-free reference configuration. In turn, we acquired in-plane stretches from the right Cauchy–Green deformation tensor, $\mathbf{C} = \mathbf{F}^{\mathrm{T}}\mathbf{F}$, and calculated the membrane tension as the force divided by the rake-to-rake distance in the deformed configuration. To characterize the resulting nonlinear tension–stretch curves, we also computed four scalar metrics: Toe Stiffness (i.e., lower region slope), Calf Stiffness (i.e., upper region slope), Transition Stretch (i.e., stretch data point nearest to the intersection of the lower and upper region slopes), and Degree of Anisotropy (i.e., the ratio between the circumferential and radial stretches at 50 N m^{-1}) (Pham et al. 2017; Jett et al. 2018; Pokutta-Paskaleva et al. 2019; Meador et al. 2020a).

2.4 Numerical experimentation

To determine the effects of heterogeneity in thickness on the biomechanics of soft tissues, we numerically analyzed mitral valve tissue samples under biaxial tension, bending, and buckling, see Fig. 2. To this end, we first identified three square areas of size 7 mm × 7 mm in the spatial thickness map of our anterior mitral valve leaflet. We then discretized these squares with shell elements and used a custom MATLAB code (MATLAB v2021b, Mathworks, Natick, MA) to map the heterogeneous thicknesses onto the shells. For the constitutive model, we chose a Neo–Hookean material with shear modulus $\mu = 20$ MPa (Rausch et al. 2013). Subsequently, we imported the discretized geometries into ABAQUS/Standard (Dassault Systemes, Providence, RI) and analyzed them under biaxial stretch, bending, and buckling using the finite element method. To biaxially test the samples, we simultaneously applied a stretch of 1.5 to all four edges of the domains. For the bending analysis, we clamped one edge of our domains and applied a moment $M = 4 \times 10^{-2}$ Nm to the opposite edge (Hughes and Liu 1981). To model the buckling response of the samples, we used a linear perturbation analysis in ABAQUS. Here, we clamped the edges of our sample and applied a pressure load of $P = 0.2$ MPa to the bottom surface of our domains as

boundary conditions (Evkin and Lykhachova 2019). Finally, we repeated these simulations but assumed that the samples had homogeneous, average thickness distributions rather than the true, spatially varying thickness distributions.

2.5 Statistics

To test whether our profilometry protocol affected the biomechanics of our test samples, we compared four mechanical metrics before and after applying the protocol. Because the mechanical tests were performed on the same samples, we used a two-sided, dependent Student *t*-test. We conducted these statistical analyses in MATLAB where we assumed that a p value smaller than 0.05 would be significant. Where applicable, we reported values as mean ± 1 standard deviation.

3 Results

3.1 Optical profilometry yields a continuous, high-resolution thickness map of an anterior mitral valve leaflet

We successfully applied the powder strategy to our test sample and obtained a continuous, high-resolution thickness map of an anterior mitral valve leaflet, see Fig. 3. That is, our contrast technique successfully enabled the autofocus-based thickness mapping of the profilometer. Additionally, we found that profilometry-derived thickness values matched the gold-standard technique (i.e., a thickness gauge) very well, see Fig. 4. Specifically, the difference between the two methods was 10 ± 27 µm, equivalent to a mean error of 1.26%.

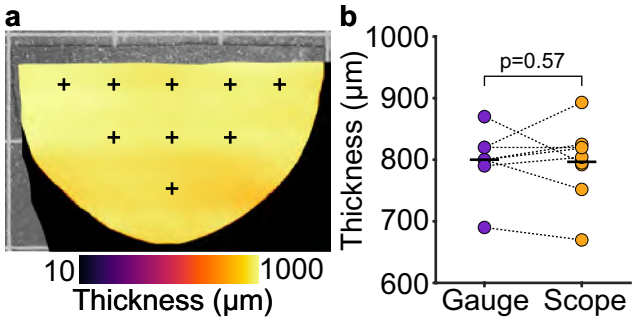

Fig. 4 Validation of our optical profilometry technique against digital thickness gauge measurements of a rubber sample. Please note, "+" demarcates the gauge measurement points and thickness data are mapped to a logarithmic scale

3.2 Our profilometry protocol does not change the mechanical properties of anterior mitral valve leaflets

To evaluate the effects of our profilometry protocol on tissue mechanics, we equibiaxially tested $n = 6$ square samples from anterior mitral valve leaflets in a dependent experimental design (i.e., repeated testing of the same samples before and after using the profilometry protocol). We found that all samples, before and after applying the profilometry protocol, exhibited classic nonlinear J-shaped loading behavior, as expected for collagenous tissues, see Fig. 5a and b. Qualitatively, the stress-stretch curves in radial and circumferential directions looked identical between both groups. Additionally we quantified the Toe Stiffness, Calf Stiffness, Transition Stretch, and Degree of Anisotropy. When comparing those values, we found no statistically significant differences in any of the metrics, see Fig. 5c. Overall, our profilometry protocol appeared to not affect our tissues' mechanics.

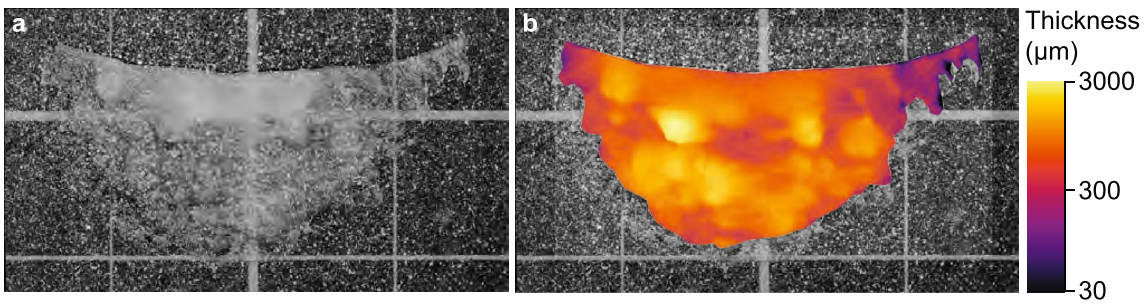

Fig. 3 High-resolution thickness map of an anterior mitral valve leaflet via optical profilometry. **a** Raw image of an anterior mitral valve leaflet with talcum powder. **b** Raw image with profilometry-based thickness map superimposed. Please note, thickness data are mapped to a logarithmic scale

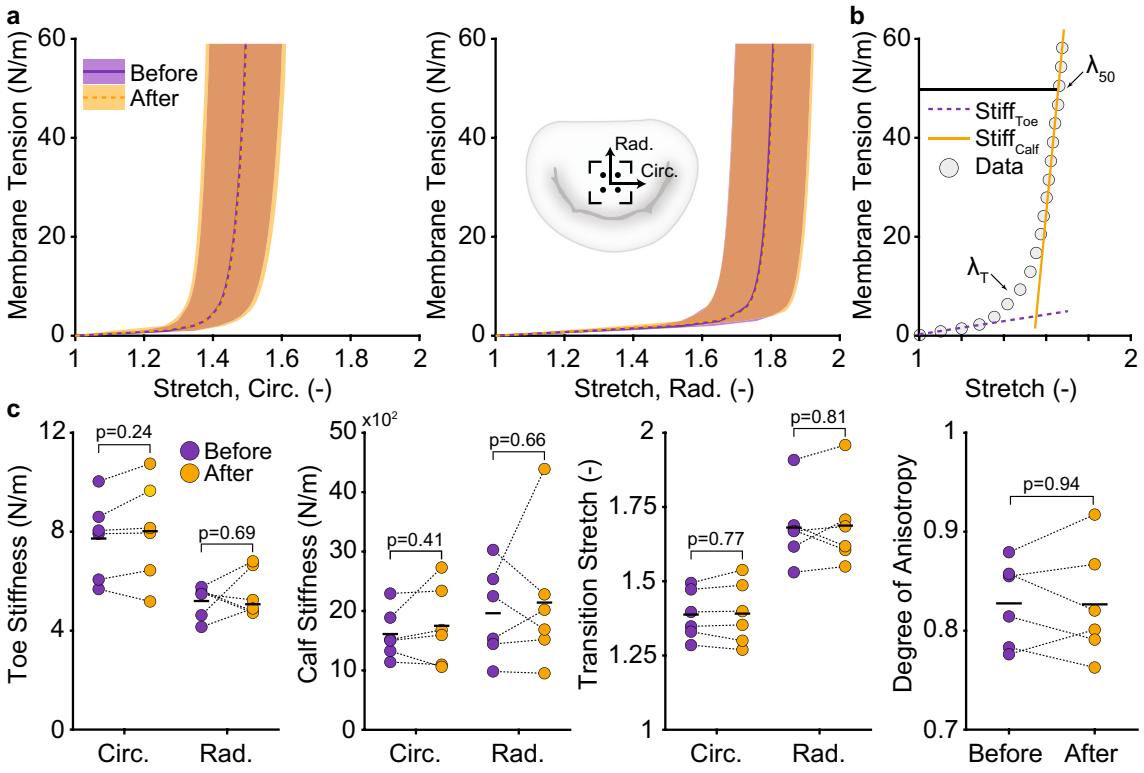

Fig. 5 Our profilometry protocol does not affect the biaxial mechanics of anterior mitral valve leaflets. **a** Tension–stretch curves in circumferential and radial direction before and after applying talcum powder and dehydrating for 10 minutes. **b** Explanation of four quantitative metrics of the biaxial tissue mechanics: Toe Stiffness (Stiff$_{Toe}$), Calf Stiffness (Stiff$_{Calf}$), Transition Stretch (λ_T), and Degree of Anisotropy (λ_{50} in circumferential direction divided by λ_{50} in radial direction). **c** Quantitative comparison of the biaxial mechanics of anterior mitral valve leaflets before and after applying our profilometry protocol

3.3 Assuming homogeneity accrues significant errors in the biaxial response of an anterior mitral valve leaflet

To determine the effects of spatially varying thickness on soft tissue biomechanics, we simulated the deformation of three anterior mitral valve leaflet samples under biaxial tension. Each sample was virtually excised from our continuous thickness map as shown in Fig. 6. In our analysis, we compared results under the assumption of thickness homogeneity to results obtained with the true, spatially varying thickness distributions, see Fig. 7. First, we found that reaction forces varied based on where the samples were excised. In other words, thickness heterogeneity induced intra-subject variability. Additionally, for a given sample we found that the assumption of homogeneity overestimated material stiffness when compared to the samples with heterogeneous thicknesses. Moreover, thickness heterogeneity induced anisotropy in the mechanical response of our tissues, even when using an isotropic material model. Together, errors in the predicted tension–stretch behavior of our samples due to the assumption of homogeneity were as large as 21% depending on sample location and material direction. Of course, we also found that predicted stresses varied spatially when considering thickness heterogeneity, while the assumption of homogeneity led to homogeneous stress fields, see Fig. 6. Quantitatively, we found stress distributions across all finite elements in our heterogeneous samples of 50 ± 20 MPa in Sample 1, 52 ± 19 MPa in Sample 2, and 50 ± 21 MPa for Sample 3. In contrast, each sample with homogeneous thickness had a uniform stress value of 41 MPa. In other words, errors in mean stress were as large as 26% when ignoring heterogeneity in tissue thickness. Additionally, we determined the sensitivity of the accrued errors to the magnitude of stretch and the anisotropy in each sample's material response, see Figs. 10 and 11, respectively.

3.4 Assuming homogeneity also accrues significant errors in the bending response of an anterior mitral valve leaflet

To determine the effects of spatially varying thickness on soft tissue biomechanics, we also simulated the deformation of three virtual anterior mitral valve leaflet samples under bending. To this end, we used the same virtual samples as above and simulated their mechanical response assuming homogeneity or applying true, spatially varying thickness

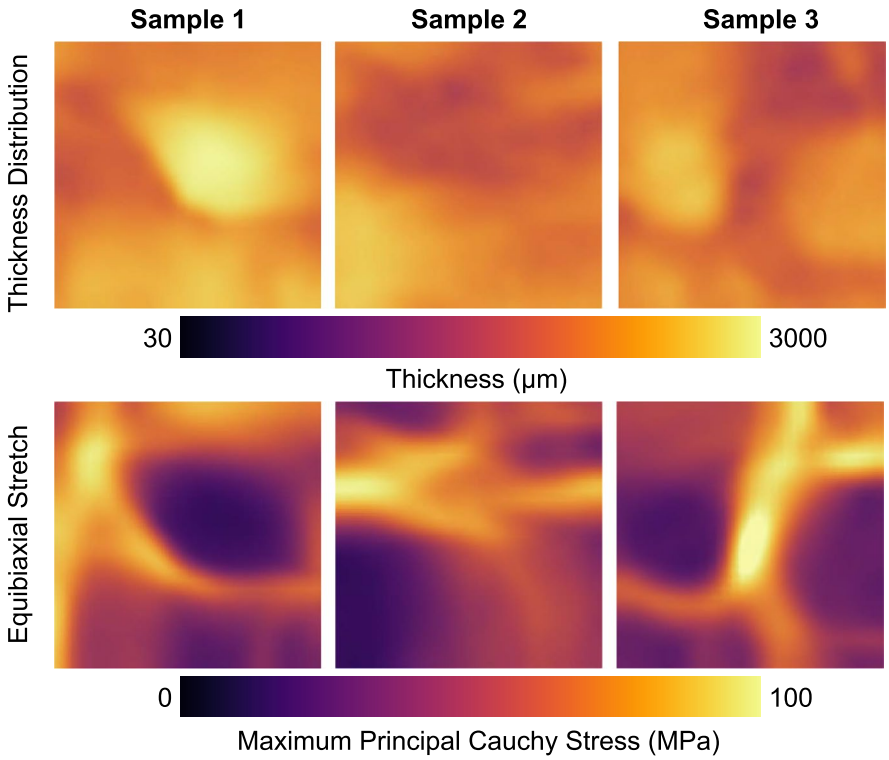

Fig. 6 Assuming homogeneity in thickness leads to significantly different material response in biaxial stretch of anterior mitral valve leaflet tissue. Stress fields vary between samples when the true, spatially varying thickness distributions are used. For reference (not shown in figure), assuming average thicknesses of 1,178.62 μm in Sample 1, 777.38 μm in Sample 2, and 792.08 μm in Sample 3 would yield a uniform stress value of 41 MPa. Please note, thickness data are mapped to a logarithmic scale

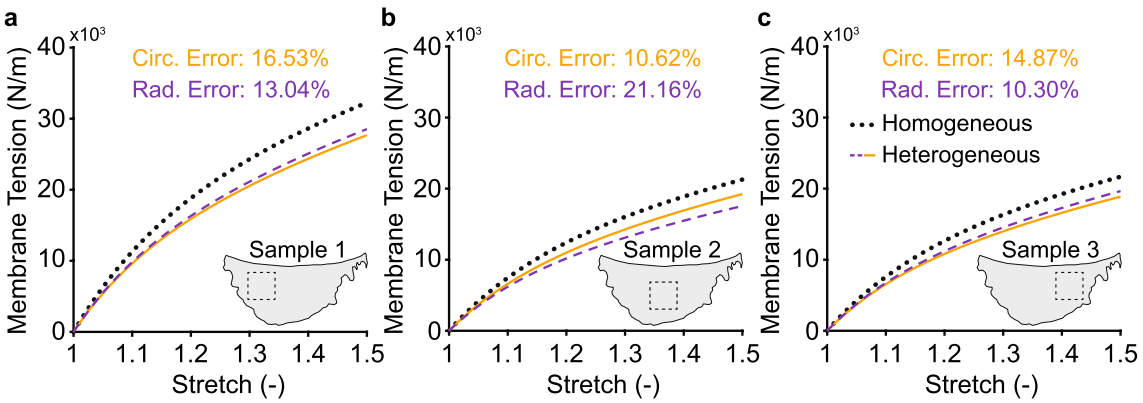

Fig. 7 Assuming homogeneity in tissue thickness leads to significant errors in the predicted constitutive response of anterior mitral valve leaflet tissue. **a–c** Predicted biaxial response of three virtual tissue samples under the assumption of homogeneity in tissue thickness versus the predicted biaxial response of the same samples with the true, spatially varying thickness distributions. Please note, "tension" is calculated as the reaction force divided by the reference edge length of 7 mm

Table 1 Assuming homogeneity in tissue thickness leads to significant errors in our tissue's bending response

Sample	Thickness	Free-edge displacement		Displacement error		Maximum principal	Stress
		X (mm)	Y (mm)	X (%)	Y (%)	Cauchy stress (MPa)	error (%)
Sample 1	Homogeneous	− 0.0217 ± 0.00174	0.472 ± 0.0174	13.2	0.64	0.77 ± 0.062	3.75
	Heterogeneous	− 0.025 ± 0.008	0.469 ± 0.031	–	–	0.8 ± 0.5	–
Sample 2	Homogeneous	− 0.246 ± 0.0171	1.57 ± 0.051	60.32	19.49	1.7 ± 0.15	32
	Heterogeneous	− 0.62 ± 0.07	1.95 ± 0.17	–	–	2.5 ± 1.61	–
Sample 3	Homogeneous	− 0.221 ± 0.0156	1.49 ± 0.049	30.94	0.67	1.68 ± 0.145	20
	Heterogeneous	− 0.32 ± 0.149	1.5 ± 0.2	–	–	2.1 ± 1.56	–

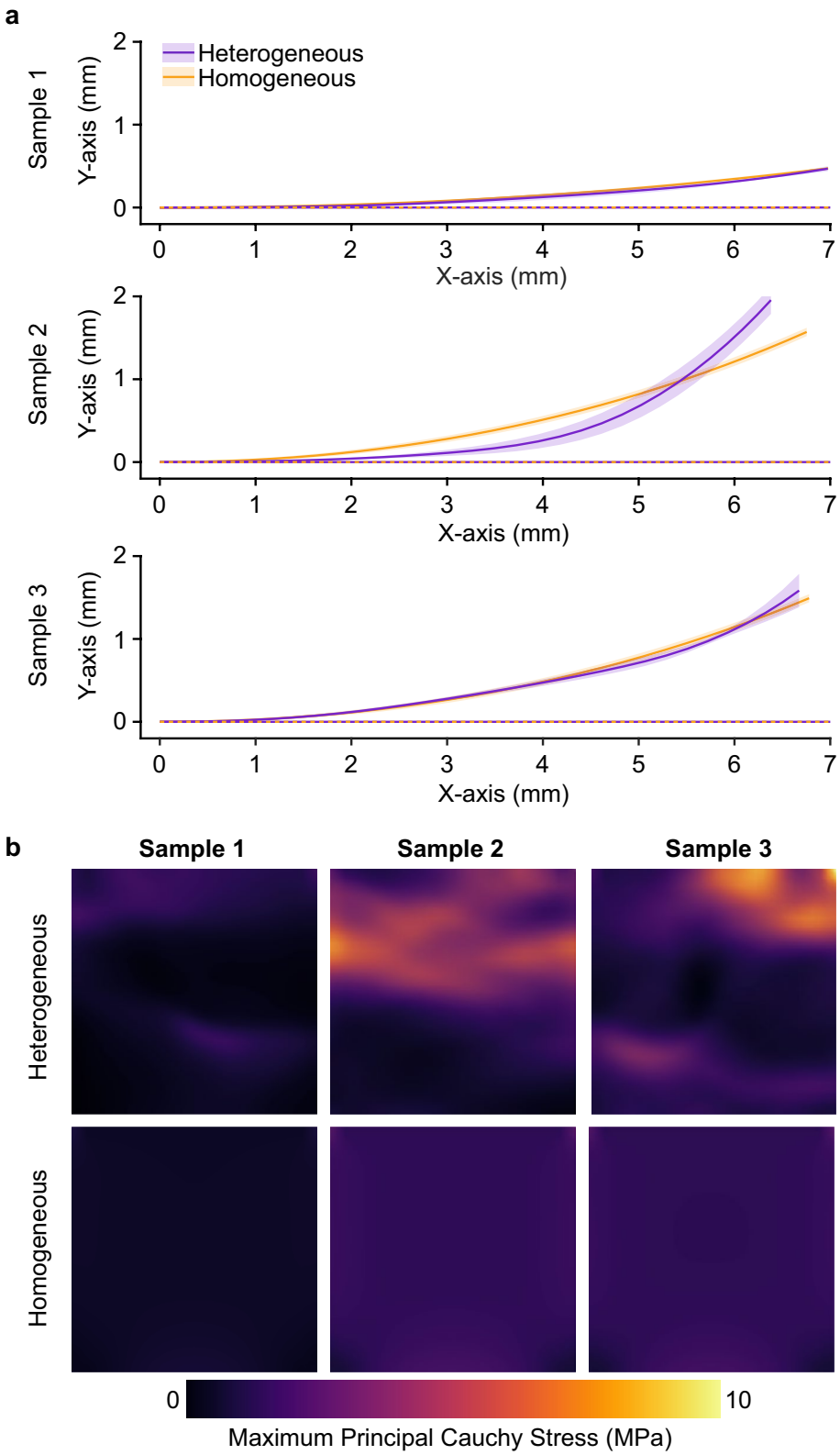

Fig. 8 Assuming homogeneity in thickness leads to significantly different material response in bending of anterior mitral valve leaflet tissue. **a** Assuming thickness homogeneity leads to artificial stiffening of samples, as evidenced by their mean bending profiles. Note that the shaded area reflects the standard deviation of the bending profile along the sample width. **b** Similarly, assuming thickness homogeneity leads to nearly homogeneous stress distributions in contrast to using the true, spatially varying thickness distributions that lead to heterogeneous stress fields

distributions. As with the biaxial tension tests, we found that the bending response varied between samples, i.e., spatially varying thickness also introduced intra-subject variability in bending stiffness. Again, as with the biaxial tension test, we found that the assumption of homogeneity overestimates the material stiffness when compared to the sample with

Table 2 Assuming homogeneity in tissue thickness leads to significant errors in our tissue's buckling response

Mode	Thickness	Eigenvalue
Mode 1	Homogeneous	10.081
	Heterogeneous	4.4375
Mode 2	Homogeneous	13.278
	Heterogeneous	4.7615
Mode 3	Homogeneous	13.278
	Heterogeneous	4.9964

heterogeneous thicknesses, see Table 1 and Fig. 8a. The resulting errors in predicted free-edge displacement were as large as 60% and 19% in the *X*- and *Y*-directions, respectively. Because bending is a heterogeneous deformation, we found spatially varying element stresses in both cases: when assuming homogeneity and when applying true, spatially varying thickness distributions, see Fig. 8b. However, we found significantly more spatial variability in the latter case than in the former case. Quantitatively, we found element stresses in our heterogeneous samples of 0.8 ± 0.5 MPa in Sample 1, 2.5 ± 1.61 MPa in Sample 2, and 2.1 ± 1.56 MPa in Sample 3. In contrast, element stresses in the homogeneous case were 0.77 ± 0.062 MPa for Sample 1, 1.7 ± 0.15 MPa for Sample 2, and 1.68 ± 0.145 MPa for Sample 3. The bending stresses and free-edge displacements are summarized in Table 1. Note, under bending, errors for mean stress were as large as 32% when ignoring heterogeneity in tissue thickness.

3.5 Assuming homogeneity also accrues significant errors in the buckling response of an anterior mitral valve leaflet

In a third test, we simulated the deformation of the anterior mitral valve leaflet in response to buckling using only one virtual sample. We repeated this simulation twice, assuming homogeneity or applying a true, spatially varying thickness distribution. As expected at this point, we found that the response between the two simulations differed, see Fig. 9. Specifically, when looking qualitatively at the first three buckling modes, we found significant deviations in the size, shape, and location of displacements. Notably, the buckling deformations of the heterogeneous sample were localized in the sample's thinnest regions. Quantitatively, we saw a divergence in eigenvalues corresponding to each buckling mode between the two cases. Specifically, the homogeneous sample buckled in the first mode at a load factor—i.e., eigenvalue—of 10.081 as compared to an eigenvalue of 4.4375 in the heterogeneous case. Moreover, for the homogeneous case, the second and third buckling modes were degenerate, they shared a common eigenvalue of 13.278, and were thus equally likely deformations. In contrast, the second and third buckling modes of the heterogeneous sample possessed distinct eigenvalues of 4.7615 and 4.9964, respectively. In other words, the second mode occurred before the third, see Table 2. Overall, ignoring heterogeneity in a buckling analysis leads to widely inaccurate results.

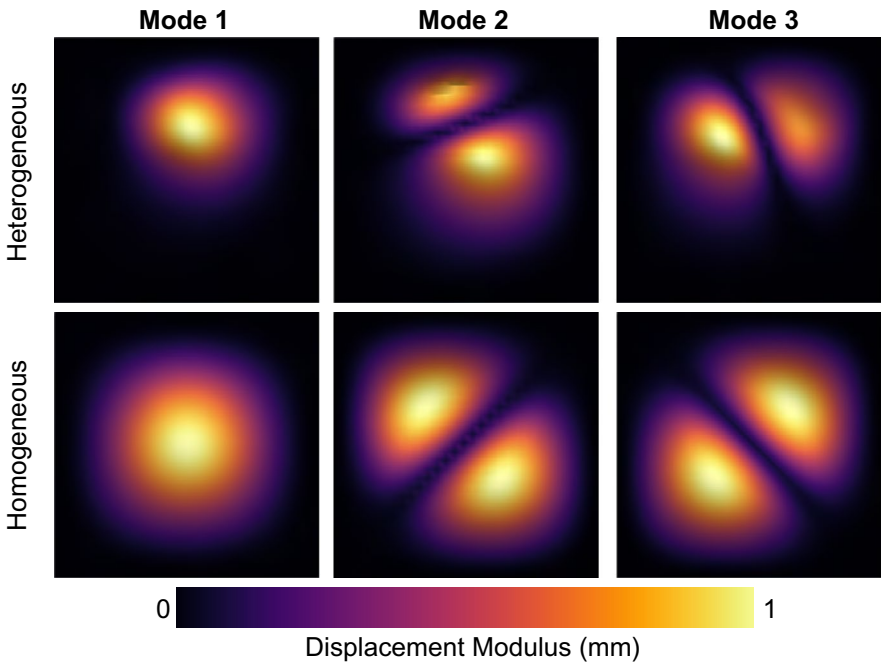

Fig. 9 Assuming homogeneity in thickness leads to incorrect predictions of the buckling modes of a clamped anterior mitral valve leaflet sample in response to a pressure load. Modes 1–3 refer to the first three predominant buckling modes. Additionally, the displacement is that out of plane

4 Discussion

Soft tissues are infamously heterogeneous. That is, their physical properties vary with location. Nonetheless, most biomechanical analyses of soft tissues ignore their heterogeneity; likely because of experimental hurdles. For example, measuring heterogeneous thicknesses of soft tissues is non-trivial. Therefore, our goal for this work was two-fold: First, our goal was to develop a technique to quickly capture non-destructive, continuous maps of soft tissue thickness under high resolution. Our second goal was to apply this technique and demonstrate the importance of considering thickness heterogeneity in biomechanical analyses of soft tissues.

We accomplished our first goal using an optical profilometry microscope. Specifically, we showed that soft tissues speckled with talcum powder provide enough contrast to optically create continuous, high-resolution thickness maps. Importantly, this imaging protocol is fast, taking only ten minutes for a 3.8 cm^2 sample at 50× magnification (Pearce et al. 2022). We also demonstrated that this technique does not affect the mechanics of the tissue by repeated biaxial tests before applying our imaging protocol and after. Lastly, we successfully validated our findings against a mechanical thickness gauge. Together, our technique overcomes the shortcomings of other, more traditional methods such as optical coherence tomography, histology, echocardiography, or thickness gauges.

We accomplished our second goal by using a representative thickness map to conduct virtual mechanical tests. Specifically, we virtually excised three square samples from the high-resolution thickness map of an ovine anterior mitral valve leaflet. On these samples, we conducted planar biaxial tests, bending tests, and a buckling analysis. Please note that we chose these deformations as representative in-vivo loading modes of mitral valve tissue (Sacks and Yoganathan 2007; Rausch et al. 2013). Importantly, for each analysis, we compared the predictions when assuming a homogeneous thickness or using the true, spatially varying thickness map. We found that assuming homogeneity can lead to widely inaccurate predictions under all three deformation modes. Most surprising to us was the magnitude of errors that could be accrued; ranging from 21% under biaxial tension up to 60% under bending. Such errors likely exceed many other effects, including disease or treatment effects, and could thus mask important findings in biomechanical analyses.

Together, accomplishing our two goals represents an important contribution to the soft tissue biomechanics literature. That is, while most of us likely expected that we should include thickness heterogeneity in our analyses, the magnitude of errors we accrue by assuming homogeneity was surprising to us. Combined with our tangible and easy imaging protocol, we hope to not only inspire but also enable others to include thickness heterogeneity in their future biomechanical analyses. It should also be noted that our speckling protocol is not only useful when being used in combination with a Keyence scope, but can likely also be applied to other, laser-based thickness measurement techniques.

Of course, our work, like all others, is subject to limitations. Most importantly, we tested our protocols against only one type of soft tissue: ovine anterior mitral valve leaflet. Thus, others may repeat similar analyses as ours on their favorite soft tissue. However, we would like to highlight that our tissue of choice represents other tissues well in that it is highly hydrated, highly collageneous, semi-transparent, and, of course, soft (Hasan et al. 2014). In other words, we believe our tissue represents other tissues reasonably well. Also, please note that we demonstrated the importance of heterogeneous thickness maps using only virtual means. We did so because it allowed us to directly contrast the assumption of homogeneity against using true, spatially varying thickness maps, which would not be possible experimentally. However, that also means that our findings are subject to the usual limitations of computational simulations. For example, we modeled our materials as hyperelastic and ignored time-dependent, viscoelastic effects, etc. (Holzapfel et al. 2001). Finally, we only considered one type of heterogeneity in our current work: that of thickness. Of course, our tissue likely also demonstrates other forms of heterogeneity, for example in stiffness. We will explore the importance of heterogeneity in stiffness similarly to this current work in the future.

In conclusion, we introduced a non-destructive, fast method to obtain continuous, high-resolution thickness maps of soft tissues. We validated our technique against thickness gauge measurements and demonstrated this technique on an ovine anterior mitral valve leaflet. Importantly, we also showed that our imaging protocol does not affect the mechanics of soft tissues. Finally, we used our high-resolution thickness map of an ovine anterior mitral valve leaflet to demonstrate the importance of including thickness heterogeneity in biomechanical analyses. Thereby, we showed that assuming homogeneity accrues significant errors under all three deformation modes. Thus, we recommend that biomechanicians consider thickness heterogeneity in their future analyses and hope they will use our technique to do so.

Appendix

See Figs. 10 and 11.

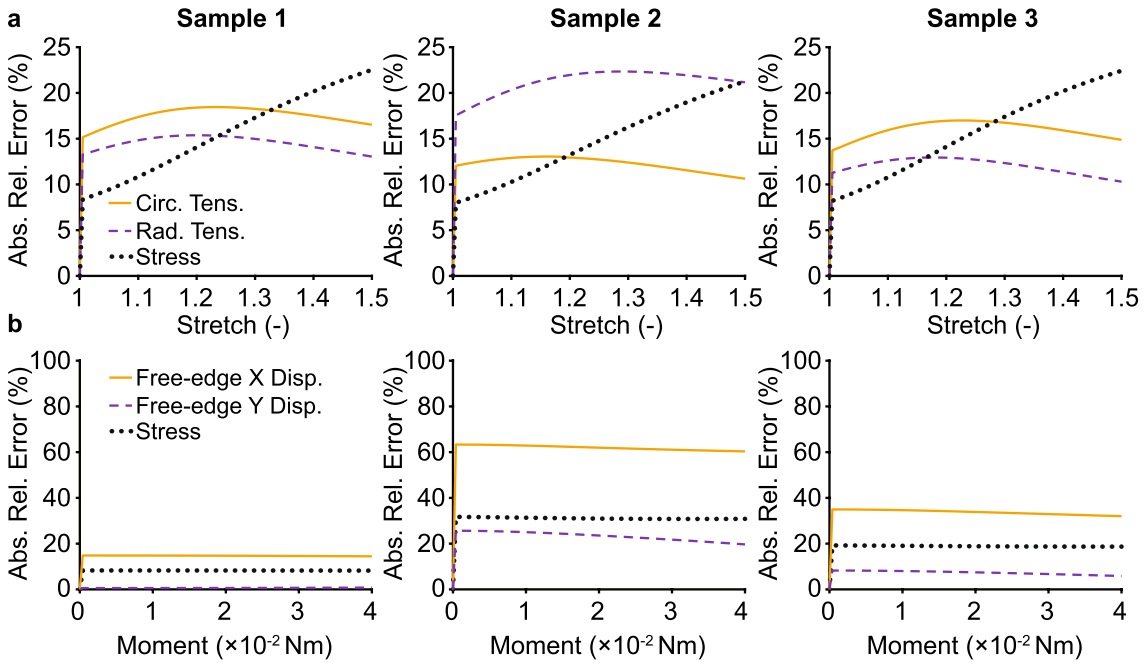

Fig. 10 The errors resulting from the assumption of thickness homogeneity are sensitive to applied stretch but not bending moment. **a** That is, under equibiaxial stretch the errors in predicted element stresses increase with applied stretch. Moreover, errors in membrane tension increase up to a stretch of nearly 1.2 and decrease thereafter. **b** In contrast, the errors under bending are mostly insensitive to applied bending moment

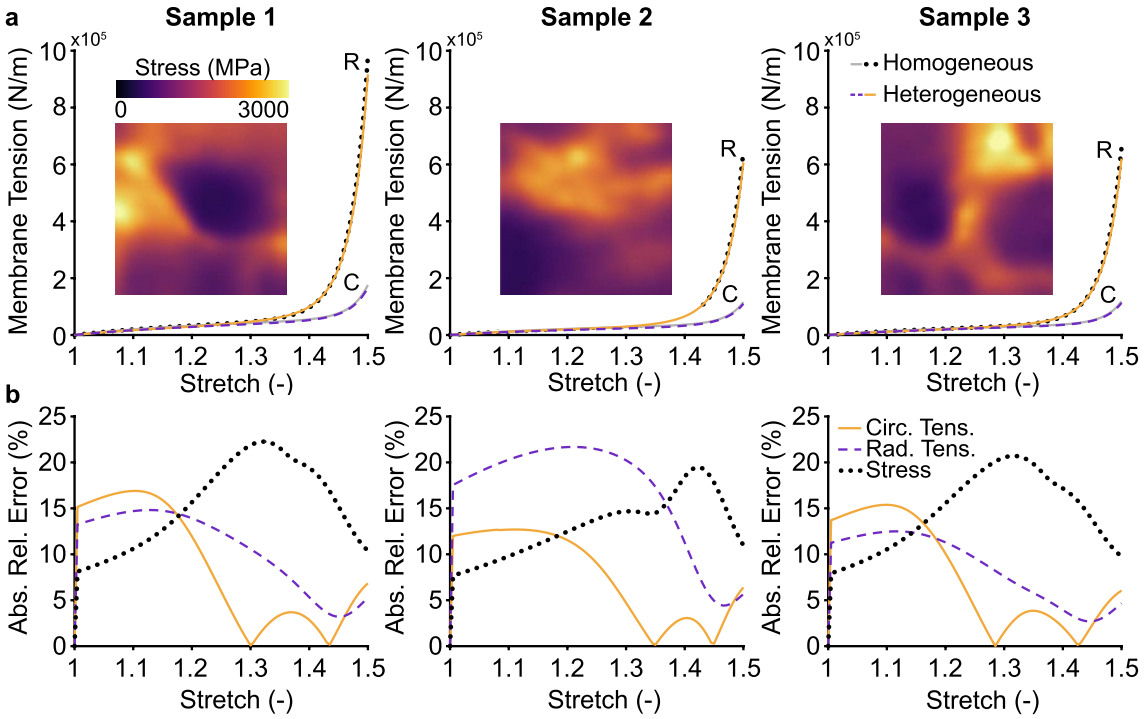

Fig. 11 Assuming homogeneity in thickness leads to significant errors under biaxial stretch of anisotropic samples too. Here, we repeated our numerical analyses using the Gasser–Ogden–Holzapfel model (as opposed to a Neo–Hookean model) with parameters $c_0 = 17.2$ MPa, $c_1 = 0.75$ MPa, $c_2 = 5.8$, and $\kappa = 0.11$ (Rausch et al. 2013). **a** Compares the tension–stretch response of three tissue samples under equibiaxial stretch assuming tissue homogeneity and using true, spatially varying thicknesses. When assuming homogeneity, all three samples generate uniform element principal stresses of 1,246.89 MPa. In contrast, true, spatially varying thicknesses lead to heterogeneous stresses as shown in the inserts. **b** Quantitatively, the error resulting from the assumption of thickness homogeneity is highly strain dependent but as large as 20% in both stress and tension. Interestingly, errors in membrane tension and element stresses are largest in the "toe" and "heel" regions of the J-shaped curve, respectively

Acknowledgements We acknowledge support by the American Heart Association through awards to Dr. Rausch (18CDA34120028) and a predoctoral fellowship to Mrudang Mathur (902502), as well as the National Institutes of Health through awards to Dr. Rausch (1R21HL 161832 and 1R01HL165251). Additionally, we acknowledge support from the National Science Foundation through awards to Dr. Rausch (2127925, 2105175, 2046148, and 1916663) and the Office of Naval Research through an award to Dr. Rausch (N00014-22-1-2073). We would also like to thank Dr. Krishnaswamy Ravi-Chandar and Jinlong Guo for their assistance with the Keyence scope. Note, the opinions, findings, and conclusions, or recommendations expressed are those of the authors and do not necessarily reflect the views of the National Institutes of Health, the National Science Foundation, or the Office of Naval Research.

Author contributions MR, MrMa, and C-YL wrote the main manuscript. MrMa and C-YL prepared all figures. MaMa and TT collected the animal tissues. All authors reviewed the manuscript.

Declarations

Conflict of interest Dr. Rausch has a speaking agreement with Edwards Lifesciences. None of the other authors have conflict of interest to disclose.

References

Aumann S, Donner S, Fischer J, Müller F (2019) Optical coherence tomography (OCT): principle and technical realization. In: Bille JF (ed) High resolution imaging in microscopy and ophthalmology: new frontiers in biomedical optics. Springer, Cham, pp 59–85

Bersi MR, Bellini C, Humphrey JD, Avril S (2019) Local variations in material and structural properties characterize murine thoracic aortic aneurysm mechanics. Biomech Model Mechanobiol 18(1):203–218

Bersi MR, Acosta Santamaría VA, Marback K, Di Achille P, Phillips EH, Goergen CJ, Humphrey JD, Avril S (2020) Multimodality imaging-based characterization of regional material properties in a murine model of aortic dissection. Sci Rep 10(1):1–23

Buerzle W, Haller C, Jabareen M, Egger J, Mallik A, Ochsenbein-Koelble N, Ehrbar M, Mazza E (2013) Multiaxial mechanical behavior of human fetal membranes and its relationship to microstructure. Biomech Model Mechanobiol 12(4):747–762

Chen S, Ní Annaidh A, Roccabianca S (2020) A microstructurally inspired constitutive model for skin mechanics. Biomech Model Mechanobiol 19(1):275–289

Duginski GA, Ross CJ, Laurence DW, Johns CH, Lee CH (2020) An investigation of the effect of freezing storage on the biaxial mechanical properties of excised porcine tricuspid valve anterior leaflets. J Mech Behav Biomed Mater 101:103438

Evkin AY, Lykhachova OV (2019) Design buckling pressure for thin spherical shells: development and validation. Int J Solids Struct 156–157:61–72. https://doi.org/10.1016/j.ijsolstr.2018.06.035

Farzaneh S, Trabelsi O, Avril S (2019) Inverse identification of local stiffness across ascending thoracic aortic aneurysms. Biomech Model Mechanobiol 18(1):137–153

Ferruzzi J, Madziva D, Caulk A, Tellides G, Humphrey J (2018) Compromised mechanical homeostasis in arterial aging and associated cardiovascular consequences. Biomech Model Mechanobiol 17(5):1281–1295

Fuentes D, Thompson E, Jacobsen M, Crouch AC, Layman RR, Riviere B, Cressman E (2020) Imaging-based characterization of convective tissue properties. Int J Hyperth 37(3):155–163

Ge Xj, Zhang L, Xiang G, Hu Yc, Lun Dx (2020) Cross-sectional area measurement techniques of soft tissue: a literature review. Orthop Surg 12(6):1547–1566

Hasan A, Ragaert K, Swieszkowski W, Selimovic S, Paul A, Camci-Unal G, Mofrad MRK, Khademhosseini A (2014) Biomechanical properties of native and tissue engineered heart valve constructs. J Biomech 47(9):1949–1963

Holzapfel GA et al (2001) Biomechanics of soft tissue. Handb Mater Behav Models 3(1):1049–1063

Hughes TJ, Liu WK (1981) Nonlinear finite element analysis of shells-part II. Two-dimensional shells. Comput Methods Appl Mech Eng 27(2):167–181. https://doi.org/10.1016/0045-7825(81)90148-1

Jana S, Lerman A (2019) Behavior of valvular interstitial cells on trilayered nanofibrous substrate mimicking morphologies of heart valve leaflet. Acta Biomater 85:142–156

Jett S, Laurence D, Kunkel R, Babu AR, Kramer K, Baumwart R, Towner R, Wu Y, Lee CH (2018) An investigation of the anisotropic mechanical properties and anatomical structure of porcine atrioventricular heart valves. J Mech Behav Biomed Mater 87:155–171

Joda A, Jin Z, Haverich A, Summers J, Korossis S (2016) Multiphysics simulation of the effect of leaflet thickness inhomogeneity and material anisotropy on the stress–strain distribution on the aortic valve. J Biomech 49:2502–2512

Lee CH, Rabbah JP, Yoganathan AP, Gorman RC, Gorman JH, Sacks MS (2015) On the effects of leaflet microstructure and constitutive model on the closing behavior of the mitral valve. Biomech Model Mechanobiol 14(6):1281–1302

Luetkemeyer CM, Rosario RA, Estrada JB, Arruda EM (2020) Fiber splay precludes the direct identification of ligament material properties: implications for ACL graft selection. J Biomech 113:110104

Luetkemeyer CM, Scheven U, Estrada JB, Arruda EM (2021) Constitutive modeling of the anterior cruciate ligament bundles and patellar tendon with full-field methods. J Mech Phys Solids 156:104577

Mathur M, Meador WD, Malinowski M, Jazwiec T, Timek TA, Rausch MK (2022) Texas TriValve 1.0: a reverse-engineered, open model of the human tricuspid valve. Eng Comput. https://doi.org/10.1007/s00366-022-01659-w

Meador WD, Mathur M, Sugerman GP, Jazwiec T, Malinowski M, Bersi MR, Timek TA, Rausch MK (2020) A detailed mechanical and microstructural analysis of ovine tricuspid valve leaflets. Acta Biomater 102:100–113

Meador WD, Sugerman GP, Story HM, Seifert AW, Bersi MR, Tepole AB, Rausch MK (2020) The regional-dependent biaxial behavior of young and aged mouse skin: a detailed histomechanical characterization, residual strain analysis, and constitutive model. Acta Biomater 101:403–413

Moran CM, Thomson AJW (2020) Preclinical ultrasound imaging-a review of techniques and imaging applications. Front Phys. https://doi.org/10.3389/fphy.2020.00124

O'Leary SA, Doyle BJ, McGloughlin TM (2013) Comparison of methods used to measure the thickness of soft tissues and their influence on the evaluation of tensile stress. J Biomech 46:1955–1960

Pearce D, Nemcek M, Witzenburg C (2022) Combining unique planar biaxial testing with full-field thickness and displacement measurement for spatial characterization of soft tissues. Curr Protoc 2(7):e493

Pham T, Sulejmani F, Shin E, Wang D, Sun W (2017) Quantification and comparison of the mechanical properties of four human cardiac valves. Acta Biomater 54:345–355

Pokutta-Paskaleva A, Sulejmani F, DelRocini M, Sun W (2019) Comparative mechanical, morphological, and microstructural characterization of porcine mitral and tricuspid leaflets and chordae tendineae. Acta Biomater 85:241–252

Rausch MK, Famaey N, Shultz TO, Bothe W, Miller DC, Kuhl E (2013) Mechanics of the mitral valve: a critical review, an in vivo parameter identification, and the effect of Prestrain. Biomech Model Mechanobiol 12(5):1053–1071

Sachs D, Wahlsten A, Kozerke S, Restivo G, Mazza E (2021) A biphasic multilayer computational model of human skin. Biomech Model Mechanobiol 20(3):969–982

Sacks MS, Yoganathan AP (2007) Heart valve function: a biomechanical perspective. Philos Trans R Soc B Biol Sci 362(1484):1369–1391

Salinas SD, Clark MM, Amini R (2020) The effects of − 80 °c short-term storage on the mechanical response of tricuspid valve leaflets. J Biomech 98:109462

Smith K, Mathur M, Meador W, Phillips-Garcia B, Sugerman G, Menta A, Jazwiec T, Malinowski M, Timek T, Rausch M (2021) Tricuspid chordae tendineae mechanics: insertion site, leaflet, and size-specific analysis and constitutive modelling. Exp Mech 61(1):19–29

Sree VD, Rausch MK, Tepole AB (2019) Linking microvascular collapse to tissue hypoxia in a multiscale model of pressure ulcer initiation. Biomech Model Mechanobiol 18(6):1947–1964

Ud-Din S, Foden P, Stocking K, Mazhari M, Al-Habba S, Baguneid M, McGeorge D, Bayat A (2019) Objective assessment of dermal fibrosis in cutaneous scarring, using optical coherence tomography, high-frequency ultrasound and immunohistomorphometry of human skin. Br J Dermatol 181(4):722–732

Witzenburg CM, Barocas VH (2016) A nonlinear anisotropic inverse method for computational dissection of inhomogeneous planar tissues. Comput Methods Biomech Biomed Eng 19(15):1630–1646

Witzenburg CM, Holmes JW (2018) Predicting the time course of ventricular dilation and thickening using a rapid compartmental model. J Cardiovasc Transl Res 11(2):109–122